ECAS 2017

sciforum

Conference Proceedings Paper

Synoptic Characteristics of the Japan Tsukuba Tornado

Ki-Hong Min[1*], Seonhee Choo[2], and Gyuwon Lee[1], and Kyung-Eak Kim[1,3]

Published: 17 July 2017

[1] School of Earth System Sciences, Major in Atmospheric Science, Kyungpook National University, Daegu, 41566, South Korea; kmin@knu.ac.kr
[2] Forecast Technology Division, Forecast Bureau, Korea Meteorological Administration, Seoul, 07062, South Korea; purehj@korea.kr
[3] Applied Meteorology Research Division, National Institute of Meteorological Sciences, Seogwipo, Jeju-do, 63568 South Korea; kimke1805@korea.kr

* Correspondence: kmin@knu.ac.kr; Tel.: +82-53-950-6360

Abstract: In this study, we conducted synoptic and mesoscale analyses to study the cause of the Japan Tsukuba tornado development, which occurred on 0340 UTC 6 May 2012. We analyzed surface and upper-level weather charts, thermodynamic diagrams and stability indices, moisture flux, SREH, isentropic analysis, PV, and Froude number to understand its development and characteristics. Prior to the tornado event, there was a circular jet stream over Japan and the surface was moist due to overnight precipitation. Circular jet stream brought cold and dry air to the upper-level and sky clearing with strong solar radiation heating the ground. A tornadic supercell developed in an area that was potentially unstable. Sounding data at Tateno showed a capping inversion at 900hPa on 0000 UTC 06 May. Strong insolation in the early morning hours and removal of the inversion instigated vigorous updraft with rotation due to vertical shear in the upper-level. This caused multiple tornadoes to occur from 0220 to 0340 UTC 6 May 2012. When comparing Tateno's climatological temperature and dew-point temperature profile with that of the day of tornado, the mid-level was moister than typical tornado sounding. This study shows that Tsukuba tornado development is due to a combination of a) topography and PV anomaly, which increased vorticity over the Kanto Plain; b) vertical shear, which produced horizontal vortex line; and c) thermal instability, which triggered supercell and tilted the vortex line in the vertical.

Keywords: tornado, supercell, instability, potential vorticity, topography

1. Introduction

Tornadoes are most frequently observed during the warm season in the U.S., but Japan in which 70% of land is covered by mountains also has an annual tornado occurrence. The Japan Meteorological Agency (JMA) published a statistical study on tornado occurrences and the subsequent damages based on 33 years of data from 1961 to 1993, and found that Japan has an annual occurrence of 20.5 tornadoes, a casualty rate of 0.58 and injury rate of 29.7 on average [1]. More recently, Matsui et al. [2] reported that the frequency of tornado occurrence changed from 2005 to 2007 compared to that of 1991 to 2004. In the latter period, the annual averaged tornado occurrence was 16.4, but in 2005 – 2007, it increased to a frequency of 26, with tornado areas concentrated in the Okinawa Islands, the West Coast, Kyushu, Shikoku, the Kanto district and the South Coast of Hokkaido. On 6 May 2012, multiple tornadoes occurred between 0300 UTC and 0500 UTC in Japan's Kanto district. Among these tornadoes, the most violent tornado rated F3 on the

Fujita scale (F-scale) occurred in the northern suburbs of Tsukuba (hereafter theTsukuba tornado) at 0335 UTC [3].

There have been numerous studies on the causes of tornado development in parts of the U.S. and Japan based on multiple aspects [4-12]. Brooks et al. [8] used the National Center for Atmospheric Research (NCAR)/National Centers for Environmental Prediction (NCEP) reanalysis data and created vertical profiles to find synoptic conditions related to severe weather thunderstorms. The study used data collected from 1997 to 1999 and discriminated environments between severe tornadic and non-tornadic thunderstorms in the eastern United States. Verbout et al. [10] compiled a 50-yr climatology (1954–2003) of significant synoptic environments related to tornado events of F2 or greater to investigate the observed tornado occurrences in valleys and plateaus. They found that most of the severe tornado events were related to the southwesterly 500 hPa flow ahead of a neutral-tilted trough. However, events with five or more significant tornadoes (tornado outbreak) were mostly related to positive-tilted troughs. This region was frequently located on the right-hand-side of a jet streak at 300 or 250 hPa, with an even split between the entrance and exit regions. Their findings indicate that significant tornado events did not necessarily favor the right-entrance or left-exit regions of a jet streak where rising motion is expected to be most intense (with straight line jet streaks). Davis and Emanuel [5] reported that the Potential Vorticity (PV) anomaly contributes 40% to creating a low-level cyclonic circulation of a mature severe thunderstorm. Gold and Nielsen-Gammon [11] studied the effect of the upper tropospheric PV on storm relative environmental helicity (SREH) and convective available potential energy (CAPE) and found that amplifying a PV anomaly reduces the SREH downshear, but increase CAPE on the counter-clockwise shear side (cyclonic) of the anomaly where the SREH impact is the largest. They concluded that deep-layer shear on the clockwise side of the PV anomaly (anticyclonic shear) is most impacted when the positive PV change increase the shear.

Niino et al. [1] conducted a statistical study to identify the spatial variability of tornadoes in Japan. They found most tornadoes occurred in coastal areas of Japan except for the Kanto Plain, which they suspected of topographical features in this area. The study failed short of reporting how the topography influenced the development of tornadoes in the Kanto Plain. Takayabu et al. [7] through a study on the 11 December 1990 tornado investigated how a low-level jet (LLJ) associated with an upper-level vortex and surface cold front caused lee cyclogenesis when traveling over the Japan central mountains (known as the Japan Alps) on the main island. A tornado formed as a meso-low developed on the lee side of the Japan Alps. Kerr and Darkow [6] examined synoptic flow environments of tornadic thunderstorms using 184 soundings closest to tornadoes. Average storm-relative wind profiles using storm velocities were obtained on the conditions of tornadic intensity, magnitude of the mean flow and CAPE, and the direction of storm motion relative to the average background flow. They reported that there is a preferred storm-relative flow structure for tornadic thunderstorms. Tornadic intensity in association with this structure appears to strengthen as 1) the magnitude of the storm-relative helicity grows through an increasingly deeper layer of the lower through mid-troposphere and 2) mid- and upper-level storm-relative winds strengthen while decreasing directional change at their heights above 4–12 km ground level.

Klemp and Rotunno [4] conducted a dynamical study on the transition of a supercell thunderstorm into a tornadic storm using a high-resolution numerical cloud model simulation with a 250 m grid resolution. They found that the low-level cyclonic vorticity increases fiercely, and the occlusion of gust front occurs rapidly as small-scale downdrafts grow next to the center of low-level circulation. As the occlusion evolves, a high-vorticity ring of air envelops the center of circulation and multiple vortex tornados are favorable of forming. A large vorticity is generated at low-level through the strong stretching and tilting of air from the storm's inflow side in the simulation. This vertical vorticity stems from the horizontal environmental shear vorticity as low-level air advances to the storm ahead of the cold outflow boundary. The rear flank downdraft intensification during this occlusion process is directed by the dynamics of strong circulation at the low-level. A high resolution numerical model simulation from Japan showed that the simulated gust front area with a

local vorticity coincides with the location of the tornado [9]. Furthermore, the location and timing of the gust front and the position of the low-level updraft associated with the meso-cyclone plays an important role in the development of supercell tornadoes. Seko et al. [12] conducted an 11-member mesoscale ensemble experiment with a horizontal resolution of 15 km using JMA's non-hydrostatic mesoscale model for two tornado events. Through the use of mesoscale ensemble prediction system and calculating the energy helicity index (EHI), CAPE, and SREH for the model output, they showed it is feasible to forecast tornadoes with an F-scale of 2 or greater.

The 6 May 2012 Tsukuba tornado developed in an environment with a strong upper-level cold air advection of -21℃ from the west and a low-level southerly warm-moist air due to a surface low pressure system located to the north [3]. There was little cloud cover during the early morning hours (0000 UTC) which allowed plenty of surface heating to occur. This created a strong instability in the planetary boundary layer (PBL) to create thunderstorms with a gust front and lightening. Eventually, multiple tornadoes broke out in the Kanto Plain between 0300 UTC and 0500 UTC. Japan Meteorological Research Institute (MRI) operated C-band polarimetric radar within 15 km of the tornado at the time of the occurrence and identified a supercell thunderstorm during the onset of the tornado [13]. Surface and Doppler radar analysis revealed that a rear flank downdraft (RFD) intensified prior to the development of the tornado, and that the tornado developed in a region south of the cross section between a convergence line and the squall line[3]. Although there have been some reports on the 6 May 2012 Tsukuba tornado with radar and microscale analyses, there has not been a thorough analysis of the synoptic and mesoscale environment which initiated instigated the development of the tornado. In this study, we conducted synoptic, thermodynamic, and dynamic analyses on the formation and development of the 6 May 2012 Tsukuba tornado in Japan.

2. Data and Analysis Method

2.1 Analysis data

To analyze the synoptic fields which caused the development of the Tsukuba tornado, we used surface and upper-level (850, 700, 500, 300 hPa) weather charts and multi-purpose Communication, Ocean and Meteorological Satellite (COMS) visible, infrared, and water vapor imagery. In addition, we analyzed the International Civil Aviation Organization (ICAO) METAR code at three nearby airports: Tokyo-Narita International Airport (RJAA: 35.46°N 140.23°E), Tokyo-Haneda International Airport (RJTT: 35.33°N, 139.47°E), and Yokota Airbase (RJTY: 35.45°N, 139.21°E).

The sounding data used in this study were taken from Tateno (36.06°N, 120.33°E) which is located 25 km southeast of the tornado. The National Aeronautics and Space Administration (NASA) Modern-Era Retrospective analysis for Research and Applications (MERRA) reanalysis data were used to further understand and analyze the dynamic and thermodynamic fields in detail [14]. The spatial resolution of the data is 0.5°× 0.7° in latitude and longitude with 72 pressure levels from 1000 hPa to 1 hPa. The MERRA data consist of hourly 2-D surface and mandatory upper-level data (dataset 1), 6 hourly 3-D atmospheric data (data 2), and 3 hourly 3-D data at a reduced resolution of 2.5°×2.5° for 72 levels. In dataset 1, there are 8 variables: horizontal wind components (u, v), specific humidity, temperature, geopotential height, ozone, and vertically integrated moisture and energy flux data.

2.2. Analysis method

On the morning of 6 May 2012, a thunderstorm developed around 0100 UTC and subsequently a tornado touched ground at 0335 UTC near Tsukuba, Japan. The timing from thunderstorm development to tornado initiation was quite short at 1~2 hours compared to the climatological timing of 6~7 hours in the Kanto Plain [15]. In this regard, we carefully analyzed possible synoptic forcing, thermodynamic and dynamic mechanisms, and the role of moisture flux in the formation and development of the Tsukuba tornado. Furthermore, we analyzed the topographic effect of the Japan Alps located west of the Kanto Plain on the onset of the tornado.

The atmospheric conditions leading to the tornado development were analyzed using surface and upper-level weather charts with special attention given to the pressure tendency, temperature distribution, and wind change. The COMS imagery was used to analyze cloud type, structure, and top, respectively. To analyze the dynamic and thermodynamic fields in detail, the MERRA data were used to recreate the 3-D atmospheric mesoscale structure during the Tsukuba tornado.

For further thermodynamic analysis, skewT–logP diagram and some additional stability indexes are used. We examined CAPE (Convective Available Potential Energy), a commonly used index for tornado outbreak, LI (Lifted Index) and SSI (Showalter Stability Index) which indicates moisture conditions for instability. Classification values for each stability index are attached in the Appendix. Due to the sparse availability for upper-air soundings every 12 hours, we generated additional soundings before and after the tornado event using the MERRA reanalysis data and calculated the stability indices.

CAPE is the largest energy that a rising parcel can have, which is calculated as follows:

$$\mathrm{CAPE} = \int_{p_n}^{p_f} (\alpha_p - \alpha_e)\, dp \qquad (1)$$

where α_e is the profile of environmental specific volume, α_p is the specific volume of a upward moving moist-adiabatic parcel from the level of free convection, p_n is the pressure at the level of neutral buoyancy, and p_f is the pressure at the level of free convection (Petty 2008). SWEAT is calculated using vertical wind shear and horizontal wind speed as follows:

$$\mathrm{SWEAT} = 12 \times T_d(850hPa) + 20 \times (TT - 49) + 2 \times WSP(850hPa) + WSP(500hPa) + SHEAR \qquad (2)$$

where T_d is the dew point temperature at 850 hPa and TT is the Total Totals Index. In the case that TT is less than 49, the value of $20 \times (TT - 49)$ is substituted by 0. $WSP(850\ hPa)$ and $WSP(500\ hPa)$ are the mean wind speed (WSP) at 850 hPa and 500 hPa, respectively, and SHEAR term is calculated from the wind shear between 500 hPa and 850 hpa. LI indicates the difference between the environmental lapse rate and the temperature of the parcel lifted from ground to 500 hPa level in the following equation:

$$\mathrm{LI} = \mathrm{T'500} - \mathrm{T500} \qquad (3)$$

where $\mathrm{T'500}$ is the temperature at 500 hPa and $\mathrm{T500}$ is the temperature of the parcel. Lower moist air and upper dry air foster unstable atmosphere conditions which can cause super-cells to develop.

The Kanto Plain, where the tornado occurred, is located on the eastern coast of Japan such that lower-level moist air easily flows inland due to the topographical features of this area. In this regard, we analyzed the lower level moisture flux convergence and calculated the 10 year mean (2002 - 2011) climatological temperature and humidity of 0000 UTC for May 1-10 and compared them with the sounding at 0000 UTC 6 May 2012 when the tornado occurred. The moisture flux convergence ($\overrightarrow{\mathrm{M}}$) is calculated as follows:

$$\overrightarrow{\mathrm{M}} = -\nabla \cdot (\mathrm{q}\, \overrightarrow{V_h}) \qquad (4)$$

where q is specific humidity and $\vec{V}_h$ is the horizontal wind vector. The equivalent potential temperature (θ_e) is very useful to determine the atmospheric stability because it contains information of both temperature and moisture of a parcel.

To study the kinematic characteristics of the atmosphere causing tornados, we investigated shear, vorticity, SREH (Storm Relative Environmental Helicity), and Potential Vorticity (PV) using the MERRA reanalysis data. A tornado develops when strong low-level shear induces horizontal vorticity, and this vorticity is tilted vertically and lifted upwards from the base. Vertical vorticity has magnitudes on the order of $1\ s^{-1}$, given typical tornado diameters on the order of 100 m [16]. Japan's Chiba tornado over the Kanto Plain in December 1990 had a vertical vorticity with a magnitude on the order of $2.0 \times 10^{-2}\ s^{-1}$ [15]. SREH is used as a proxy that calculates the dot

product of the difference between the environmental from storm velocity and the 3-dimensional vorticity as follows:

$$\text{SREH} = -\int\left(\vec{V} - \vec{C}\right)\cdot\left(\nabla \times \vec{V}\right) dz \qquad (5)$$

The motion of the storm should be observed by high-resolution observation devices like radar to determine the storm velocity. However, the purpose of this research was to investigate the synoptic and mesoscale development mechanism of the tornado; therefore, we substituted storm velocity with 1/2 of the wind speed at 500 hPa and integrated it from the surface to 3 km above ground taking into consideration the topography of Japan. A weak tornado could occur when the value of SREH is greater than 150 m^2s^{-2}, and a severe one could occur when the SREH is greater than 450 m^2s^{-2}.

PV is used to define the dynamical tropopause, for which the value varies between researchers from 1 to 3.5 PVU (PV Unit = 10^{-6} m^3 s^{-1} K kg^{-1}). Reed [17] considered 1.5 PVU, Hoerling et al. [18] 1.5 PVU, and Bithell et al. [19] 1 PVU, respectively, as the dynamical tropopause [20]. In this study, we considered a 1.6 PVU level as the dynamic tropopause and values greater than 1.6 PVU as PV anomalies from the stratosphere.

There are three mountains called the Japanese Alps in the center of Japan. The altitude of the Japanese Alps is above 2500 m, and Mount Fuji (3776 m), the highest mountain of Japan is located in the Akaishi Mountains, one of the three mountains. Although the area of the Japanese Alps is a third of the European Alps, the impact on causing cyclones is comparable to that of the European Alps [7]. Located on the western, windward side of where the Tsukuba tornado occurred, the Japanese Alps are considered to have a mechanical influence on the outbreak of tornadoes. The Froude number (Fr) is used for analyzing this cause. The Froude number is the ratio of the mean flow to the gravity wave phase speed, and mountain-induced flow can be expressed by the Froude number. The Froude number is calculated as follows:

$$Fr = \frac{U}{N\,h_m} \qquad (6)$$

where U is the mean wind-speed between the ground and the layer at 850 hPa and N is the Brunt–Väisälä frequency, assumed to be 0.01 referring to the thermodynamic diagram of Shionomisaki, Japan (33.5°N, 135.8°E), and h_m is the perturbation fluid depth, assumed to be 1000 m [7]. When Fr is greater than 1, due to the upstream propagation of gravity waves relative to the mean flow, perturbation pressure gradients of sufficient magnitude is produced to balance the nonlinear advection of downstream fluid.

3. Analysis Results

3.1 Synoptic analysis

We analyzed the upper-level and surface weather charts to determine the synoptic conditions before and after the tornado outbreak. Figure 1 represents the surface and upper-level weather chart at 300 hPa for 0000 UTC 6 May 2012. There is a cyclone with central pressure of 996 hPa located over Vladivostok, Russia, northwest of Japan just before the tornado outbreak (Figure 1(a)). This cyclone with its central pressure of 1000 hPa had been stationary since 0000 UTC 5 May because of a strong anticyclone and upper-level ridge in the Northwestern Pacific.

The 300 hPa weather chart was analyzed to examine whether the jet stream had an influence on the outbreak of the tornado. There was a circular jet stream detached from the main polar jet stream over Japan at 0000 UTC 6 May (Figure 1(d)). A jet stream detached from its main polar jet is known to advect cold air in the area beneath the circular jet stream [21]. The jet stream had already started to detach at 1200 UTC 5 May (figure not shown) and the temperature distribution of the 700 & 850 hPa chart represents this well (Figure 1(b)-(c)). In the 850 hPa weather chart, the temperature over Tsukuba decreased from about 12 °C at 1200 UTC 5 May to 9 °C at 0000 UTC 6 May, which indicates a strong influx of cold air by the circular jet stream.

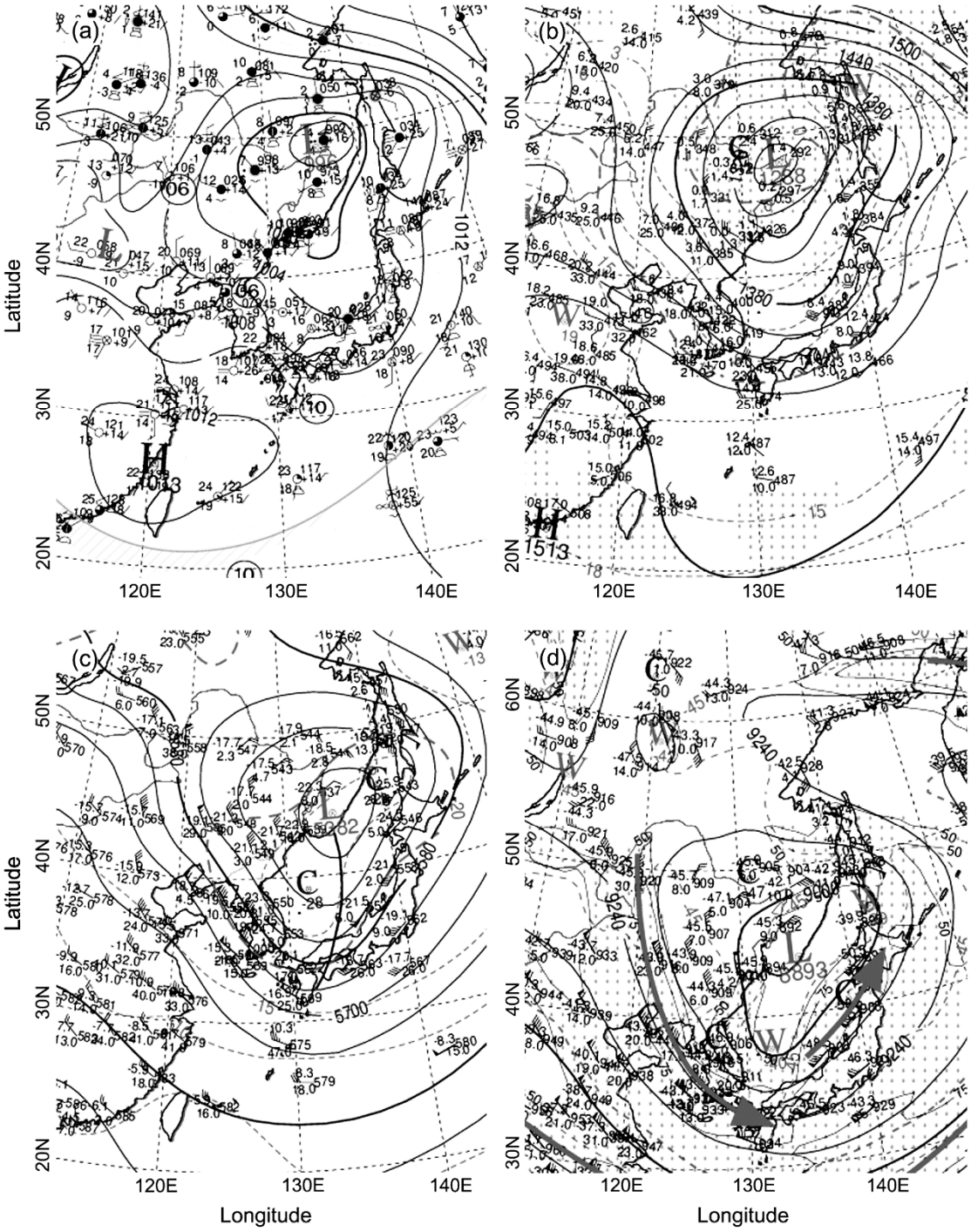

Figure 1. Weather charts for 0000 UTC 6 May 2012 at (a) the surface, (b) 850 hPa, (c) 700 hPa, and (b) 300 hPa, respectively.

The IR imaginary of COMS was used to analyze the developing process of the supercell, the mother-cloud of the Tsukuba tornado. Figure 2(a) shows the COMS imaginary at the time of the tornado outbreak at Tsukuba (0345 UTC 6 May). The existence of a circular jet stream can be seen at 0000 UTC 6 May on the COMS imaginary. The circular jet stream caused severe convective clouds to develop on the lee of the Japanese Alps after 0000 UTC 6 May, and prior to the tornado event (0340 UTC), a conspicuous supercell developed over Tsukuba as seen on the 0333 UTC image. The Tokyo Doppler radar station observed a hook echo at the time of the tornado's outbreak and identified that the tornado developed from a supercell thunderstorm [3].

On the previous surface weather chart, the central pressure of the cyclone located near the Vladivostok (43°N, 132°E) area weakened gradually with an increase of 6 hPa from 0000 UTC 5 to 0000 UTC 6 May. This contradicts the condition for developing a tornado within a super-cell; thus, we further analyzed whether the central pressure in Tsukuba also weakened. We analyzed the 3 hour pressure change in Tsukuba from the ICAO data. The time series for the wind speed and the 3 hour pressure tendency at Ibaraki Airport from 0000 UTC 5 May to 0000 UTC 7 May 2012 is shown in Figure 2(b). Solid and dashed lines represent the wind speed and pressure tendency, respectively, and the diamond represents the 1 minute wind gust. The straight solid line is the time of the tornado occurrence. The pressure gradually decreased from the morning before the tornado occurred (2300 UTC 5 May) with -1 hPa per 3 hr to the time of the tornado (0345 UTC 6 May) with -5 hPa per 3 hr and its range of decrease increased sharply. At the same time, the wind speed increased to 11 ms^{-1} with wind gusts of 18 ms^{-1} which peaked at the time of the Tsukuba tornado. Hence, we noted that although the synoptic cyclone weakened on the surface weather chart, the surface low in Tsukuba actually strengthened significantly.

Vertical wind shear plays an important role in developing a thunderstorm type in a convective environment. A hodograph represents such an environment of vertical wind shear well. Figure 2(c) is a hodograph using the sounding data of Tateno with the solid line indicating the hodograph at 0000 UTC 06, just before the tornado occurrence. The dashed line is at 1200 UTC 06 after the tornado outbreak. In general, the lower level at 0000 UTC and 1200 UTC is quite symmetric, and there is veering at 0000 UTC, and backing at 1200 UTC. This implies a cold front passed after the tornado outbreak, although it is not apparent on the weather charts. Furthermore, there is wind shear and veering at the lower-levels, but backing from 918 hPa to 519 hPa. Hence, we can identify that thermodynamic instability was high due to lower-level warm air and upper-level cold air.

The typical atmospheric humidity stratification of a tornado outbreak has a moist lower-level and a dry upper-level. To check if such structure was the case for the Tsukuba tornado, we analyzed the skewT–logP diagram (Figure 2(d)). Indeed, from the sounding data of Tateno at 0000 UTC 06, the overall structure shows the upper-level being quite dry ($T - T_d > 6^oC$), whereas the layer beneath 950 hPa is moist ($T - T_d < 6^oC$) in general. With the hodograph, we can identify veering winds and shear at the lower-levels. There was conspicuous capping inversion under 900 hPa, with an inversion top temperature of about 15 ^oC. When following the dry adiabats back to the surface, a temperature of 24 ^oC was obtained, which is the temperature needed to break the capping inversion. According to the ICAO data, the ground temperature at 0300 UTC rapidly rose to 26 ^oC, which was sufficient to break the cap.

Since stability indices are a good measure of the atmospheric capability of vertical motions, we determined various degrees of instability using CAPE, SWEAT, LI, and SSI. Table 1 presents the stability indices using the MERRA reanalysis data at the closest data point from the Tateno tornado. The stability indices at 0000 UTC 06, calculated from the radiosonde sounding data of Tateno is also included in the table. The Tateno sounding at 0000 UTC 06 indicated ‘marginally unstable’ for CAPE, ‘severe possible’ for SWEAT, ‘weak possible’ for LI, and ‘thundershowers’ for SI. All the indices indicated some possibility of severe weather [22]. Stability indices using the MERRA reanalysis data showed that CAPE, LI, and SSI were the highest at 0300 UTC just before the tornado event, but SWEAT had the lowest value among the others. The low SWEAT value at 0300 UTC could be a drawback resulting from the fact that MERRA is reanalysis data. However, it also means that vertical wind shear between 850 hPa and 500 hPa was weak. This coincides with the hodograph at 0000 UTC 06 (Figure 2(c)), where there is strong backing between 850 hPa and 500 hPa, but wind shear between 850 hPa and 500 hPa is not strong. When comparing LI and SSI at the same location, the LI represented the situation well in that a tornado occurred, but SSI generally did not with its value being the highest at 0300 UTC. This means that the dew point below the 850 hPa level was higher than that above, i.e. the lowest level was very moist.

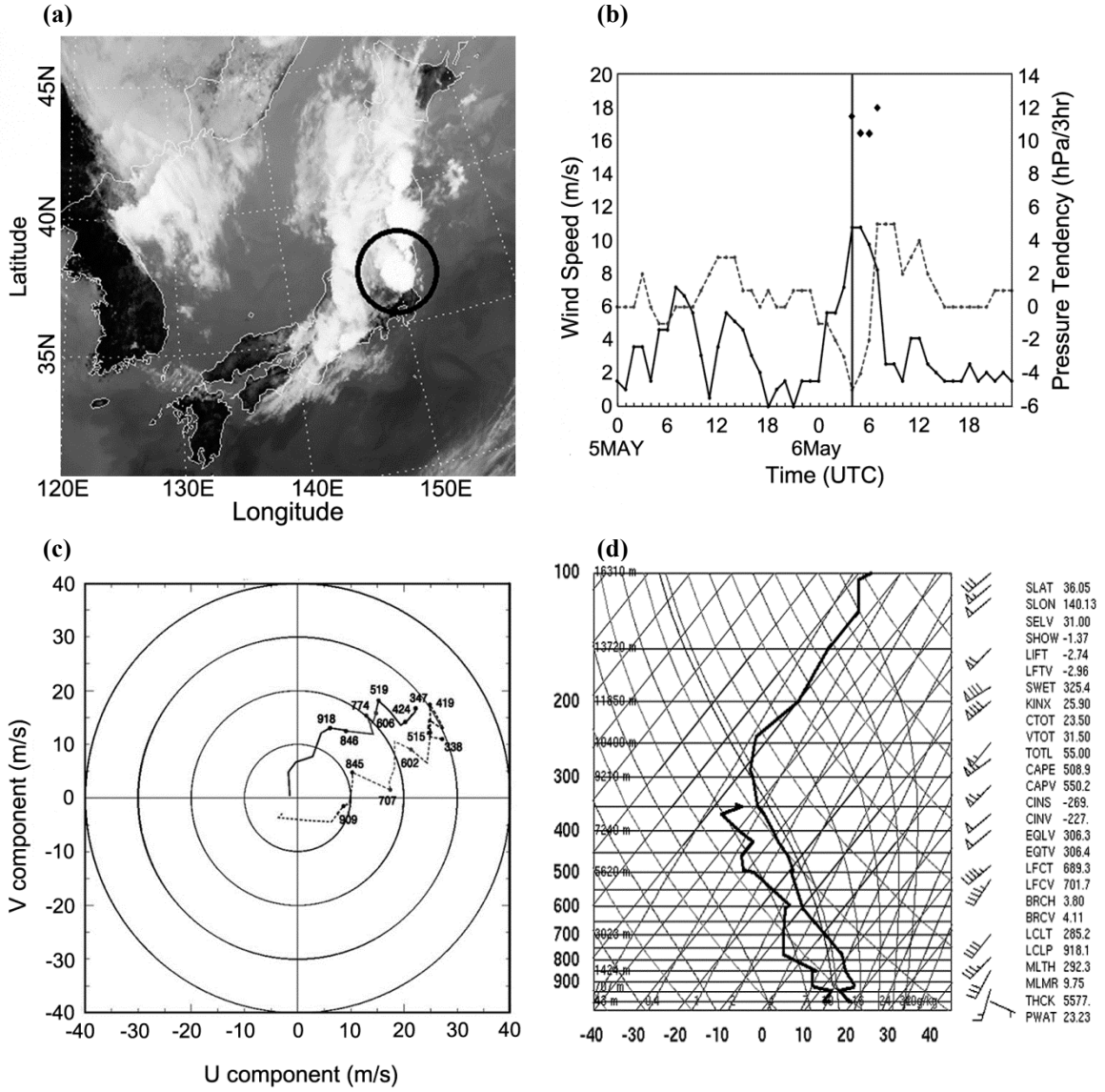

Figure 2. (a) COMS IR image at 0345 UTC 6 May 2012. Open circle represents the tornadic supercell cloud. (b) Time series of wind speed (solid line) and 3 h pressure tendency (dashed line) at Ibaraki Airport from 0000 UTC 5 May to 0000 UTC 7 May 2012. Black dots are wind gust speed and thick solid line represents the time of tornado. (c) Hodograph of 0000 UTC (solid line) and 1200 UTC (dashed line) 6 May 2012, respectively. (d) SkewT–logP diagram at Tateno for 0000 UTC 6 May 2012.

Table 1. Stability indices calculated with the MERRA data from 0000 UTC to 0600 UTC 6 May 2012 at Tateno. The values in the parenthesis are from the 0000 UTC radiosonde data.

	0000 UTC 6	0300 UTC 6	0600 UTC 6
CAPE ($J\,kg^{-1}$)	656 (508.9)	1226	1143
SWEAT	255.32 (325.4)	166.27	180.91
LI	-3 (-2.74)	-5	-4
SI	2.14 (-1.37)	3.64	2.02

3.2 Moisture and thermodynamic analyses

When the moist atmosphere encounters dry air, moist air mixed with dry air can soar and a supercell develops in these conditions. We analyzed the moisture flux at the surface to determine the inflow of water vapor and investigated the precipitation using the GPCP data for the precipitation between 1200 UTC 5 May and 0600 UTC 6 May (figure not shown). Moisture flux between 1800 UTC 5 to 0300 UTC 6 May, showed that the water vapor over the main island of Japan increased. Precipitation started at 1800 UTC 5 over the Japan Alps and extended eastward to the main island of Japan even after the tornado outbreak. Hence, we note that the ground was wet adding moisture to the atmosphere when the tornado occurred, and the sky clearing provided sensible heat to the atmosphere, which aided in the development of a tornadic supercell.

When there is a big difference in the water vapor amount or equivalent potential temperature between the upper- and lower-level, convection can easily occur. Figure 3 represents the east-west and north-south cross sectional diagram of equivalent potential temperature (θ_e) for 0000 and 0300 UTC May 6 May. Both cross sectional diagrams show that the atmosphere was considerably unstable at 0000 UTC, and became even more unstable at 0300 UTC just before the tornado outbreak. The equivalent potential temperature decreased from 335 K to 315 K below 600 hPa in the east-west cross sectional diagram (Figure 3(a) & (b)). The decrease is also evident in the north-south cross sectional diagram at 0300 UTC (Figure 3(d)). Overall, the atmosphere was very moist from the surface to 600 hPa, and dry air intrusion above increased the thermodynamic instability of the environment.

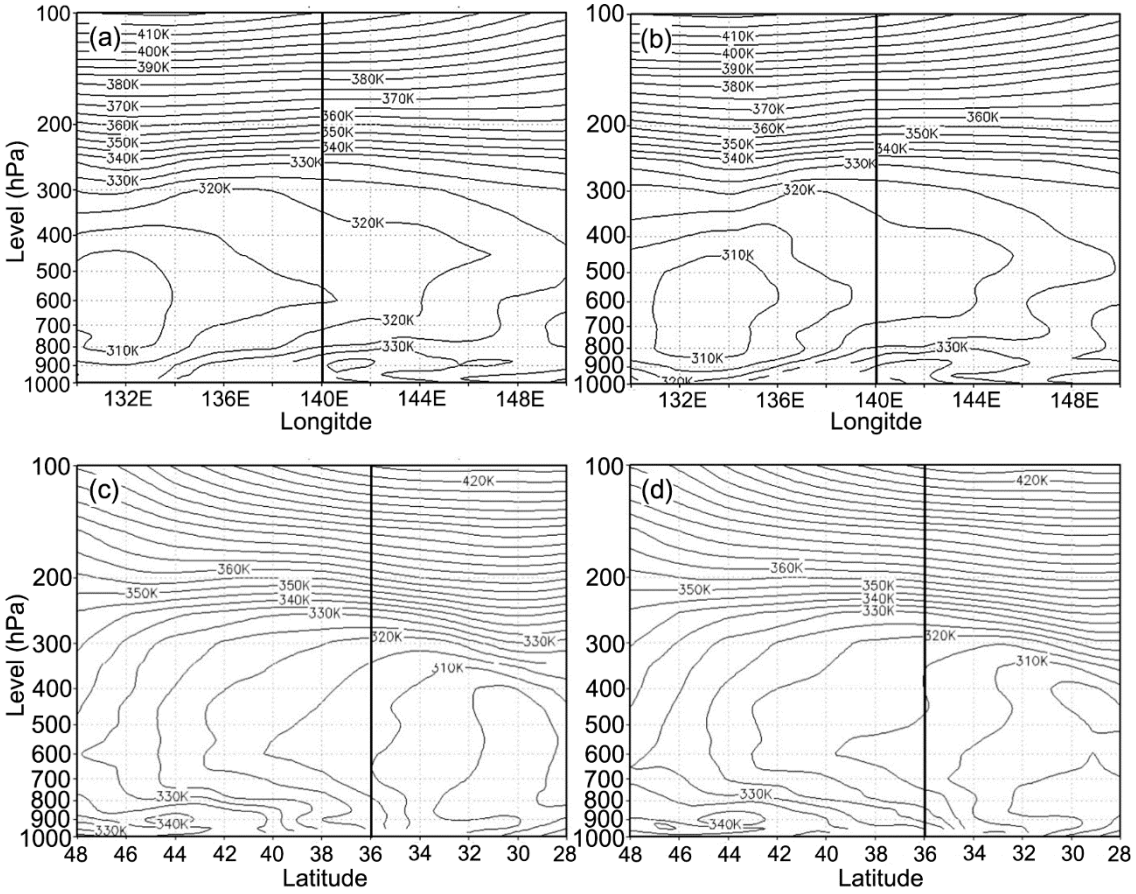

Figure 3. Vertical cross section of the equivalent potential temperature (θ_e) along the zonal direction at 139.25°E (top panel) and meridional direction at 35.625°N (bottom panel) from (a, c) 0000 UTC to (b, d) 0300 UTC 6 May 2012, respectively. The dark straight line represents the time of tornado occurrence.

Recall that the skewT-logP diagram of Tateno was very moist compared to the typical U.S. tornado soundings. In the US, low-level moisture and instability is weaker and capping inversion is located at a higher level when compared with the Tateno sounding. Thus, there needs to be strong solar radiation and a buildup of instability for a tornado to occur, whereas in the case of Japan, the lower-level was very moist and instability was strong such that it was easier for a cap to be broken even with a small variation in the temperature, which is in sharp contrast to the U.S.

In this regard, we generated a 10-year mean climatological profile using temperature and the dew point temperature in Tateno, and compared it with values for the 0000 UTC 6 May 2012 sounding when the tornado occurred. Figure 4(a) shows the vertical profile on the day of the tornado outbreak (red line) and its climatological mean (blue line). Figure 4(b) shows the dew-point depression for climatological mean and on the day of the tornado outbreak as in Figure 4(a). The capping inversion is evident in Figure 4(a) and is located below the 850 hPa level, and the slope of the sounding is steeper than that of the climatological profile. Figure 4(b) shows there was a moist layer close to the surface at 0000 UTC 6 May, but the dew point depression above 700 hPa was quite dry compared to normal conditions. Because of the strong thermodynamic instability, the tornado developed within 1~2 hours of the initiation of the supercell. Shimizu et al. [23] studied a supercell-like storm in the Kanto Plain on 24 May 2000, which developed in a moist environment. The study found that although humidity under the melting layer was as high as 60 ~ 90 %, a supercell-like storm could occur in mid-level moist condition with features such as strong vertical vorticity, hook echo, and significant updraft similar to that found in a dryer environment.

3.3 Dynamic analysis

We analyzed the surface and 850 hPa wind shear from 1800 UTC 5 to 0300 UTC 6 May to determine the presence of vertical shear, which can trigger a horizontal roll like rotation or vortex line (Figure 5). When comparing the wind vectors at the surface (red arrow) to 850 hPa (yellow arrow), the closer it was to the time of the tornado outbreak, the stronger the shear was. The surface wind over Tsukuba turns clockwise from 1800 UTC 5 to 0300 UTC 6 May, indicating that warm air advection was present as seen in the previous hodograph.

Storm relative environmental helicity (SREH) provides an indication of an environment that favors the development of thunderstorms with rotating updrafts. High values of SREH (> 150 m^2s^{-2}) are usually associated with long-lived supercells with rotating updrafts, capable of producing tornadoes (Bunkers et al., 2000). Figure 6 shows the SREH calculated from the MERRA data from 0000 UTC to 0600 UTC 6 May 2012. Values over Tsukuba were 330, 420, and 480 m^2s^{-2} from 0000 UTC to 0600 UTC 6 May, respectively. Considering that a weak tornado could occur when the SREH is greater than 150 m^2s^{-2}, the SREH over Tsukuba was very large.

In addition, we examined the PV anomaly and potential temperature to analyze the role of upper-level dynamics in initiating a tornado outbreak. Figure 7 shows the east-west cross section at 40°N for 1800 UTC 5 to 0300 UTC 6 May 2012 with the long dashed line indicating the potential temperature; the solid line is for PV, and the heavy solid contour indicates a dynamic tropopause of 1.6 PVU. The approach of the PV anomaly and lowering of the dynamic tropopause from 2100 UTC 05 to 0600 UTC 06 May is clearly seen with values of 0.6 PVU close to the surface. As the 1.6 PVU approached Tsukuba, we can see stretching of isentropic contours ahead of the tropopause folding. We noted that the dynamic tropopause is situated between 310~320 K isentropic surfaces. Based on this, we further analyzed the distribution of the PV anomaly on the 315 K isentropic surface (Figure 8). In the figure, the short dashed line indicates PV; the long dashed line is the pressure level, and the thick dashed line indicates the dynamical tropopause of 1.6 PVU. The zonally oriented PV anomaly at 1200 UTC 5 May, quickly makes a positive tilt along the southwest to northeast direction and eventually becomes meridional at 0600 UTC 6 May. The relatively fast approaching PV anomaly at latitudes below 40°N, induced cyclonic circulation and provided a favorable environment for a tornado to occur.

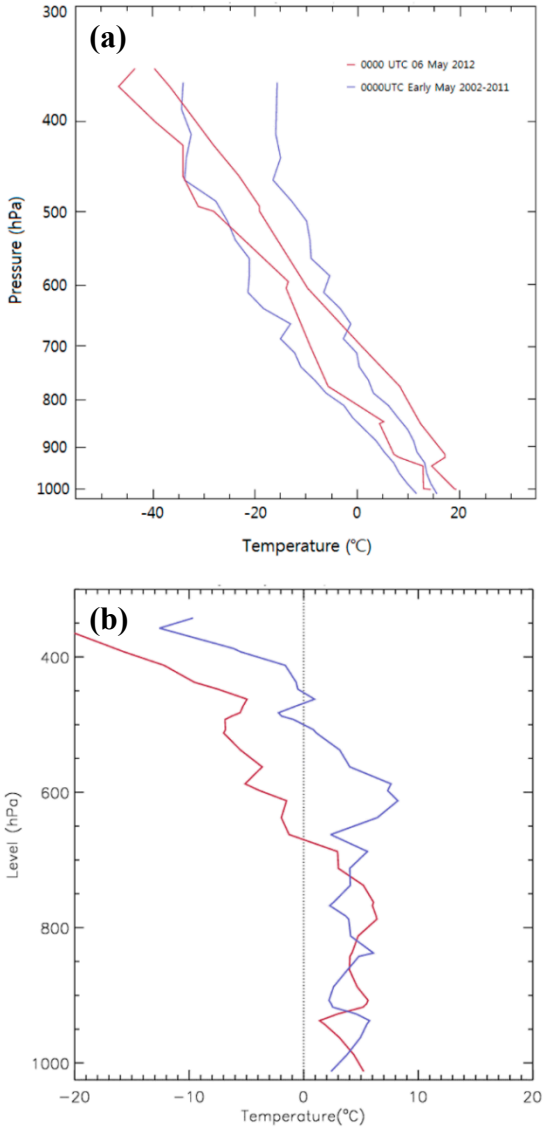

Figure 4. Vertical profile of (a) temperature with the dew-point temperature and (b) dew-point temperature depression at Tateno. Red line represents 0000 UTC 6 May 2012 and blue line represents the 10-year mean climate.

Lastly, to investigate the topographical influence on the Tsukuba tornado, we analyzed 850 hPa vorticity with topography shaded in color (Figure 9). The green and yellow areas indicate the Japan Alps which has an altitude of approximately 2500 m. Tsukuba is located on the leeward side of the Japan Alps and Tsukuba Mountain of 770m is located the northeast of the Kanto plain. Overall, the change of vorticity was small in most areas, but there was a steady increase in vorticity from 4.0×10^{-5} to $1.0 \times 10^{-4}\ s^{-1}$ on the lee of the Japan Alps and Kanto Plain. Note that the winds at 850hPa were mainly from the southwest and hence, shrunken parcels over the Japan Alps were stretched after passing the mountains increasing the vorticity up to one order of magnitude larger than the windward side. The Froude number was calculated and is presented in Table 2. The Froude number increased with time from 1500 UTC 05 to 0000 UTC 06, and was greater than 1 after 1800 UTC 05 for 850 hPa. This indicates that the flow indeed moved over the mountain and allowed the vortex to be stretched which aided in the development of the tornado.

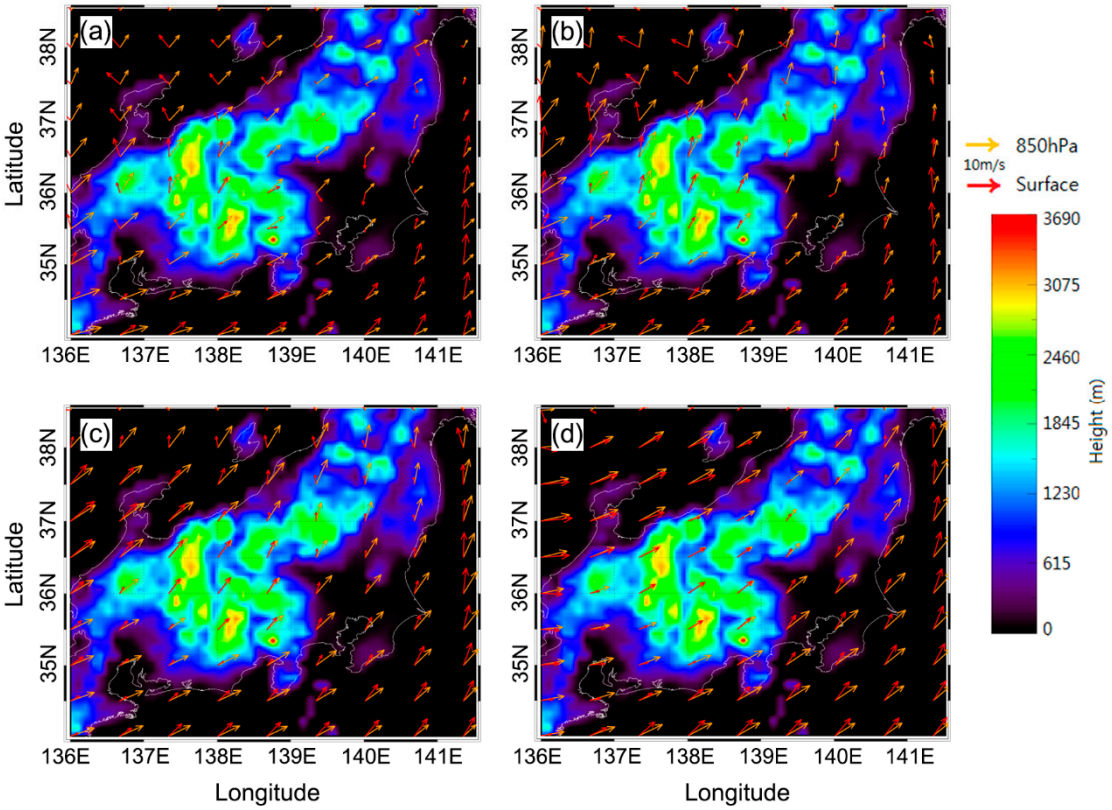

Figure 5. Surface (red) and 850 hPa (orange) wind vectors from the MERRA data with terrain height given in the background for (a) 1800 UTC 5, (b) 2100 UTC 5, (c) 2100 UTC 5, and (d) 0300 UTC 6 May 2012, respectively. The scales for the 10 ms^{-1} wind vector are shown in the upper right corner.

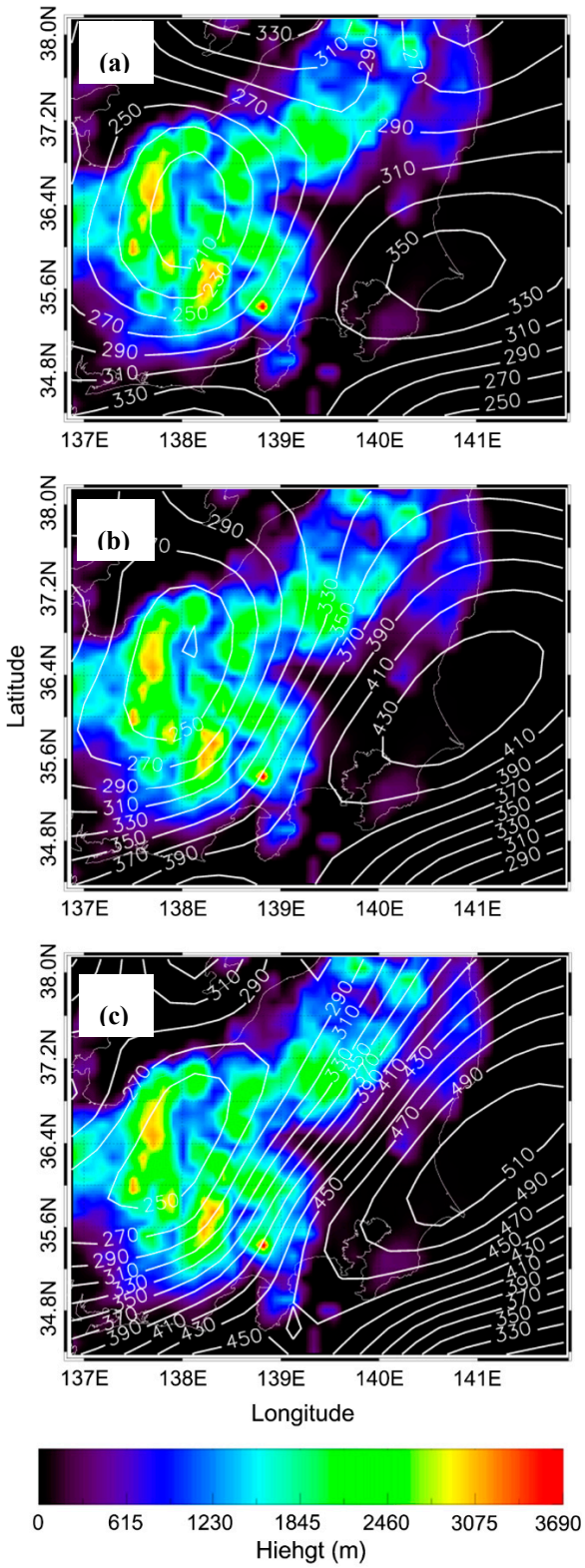

Figure 6. Storm relative helicity calculated from the MERRA data for (a) 0000 UTC, (b) 0300 UTC, and (c) 0600 UTC 6 May 2012, respectively. Units are in [m^2s^{-2}].

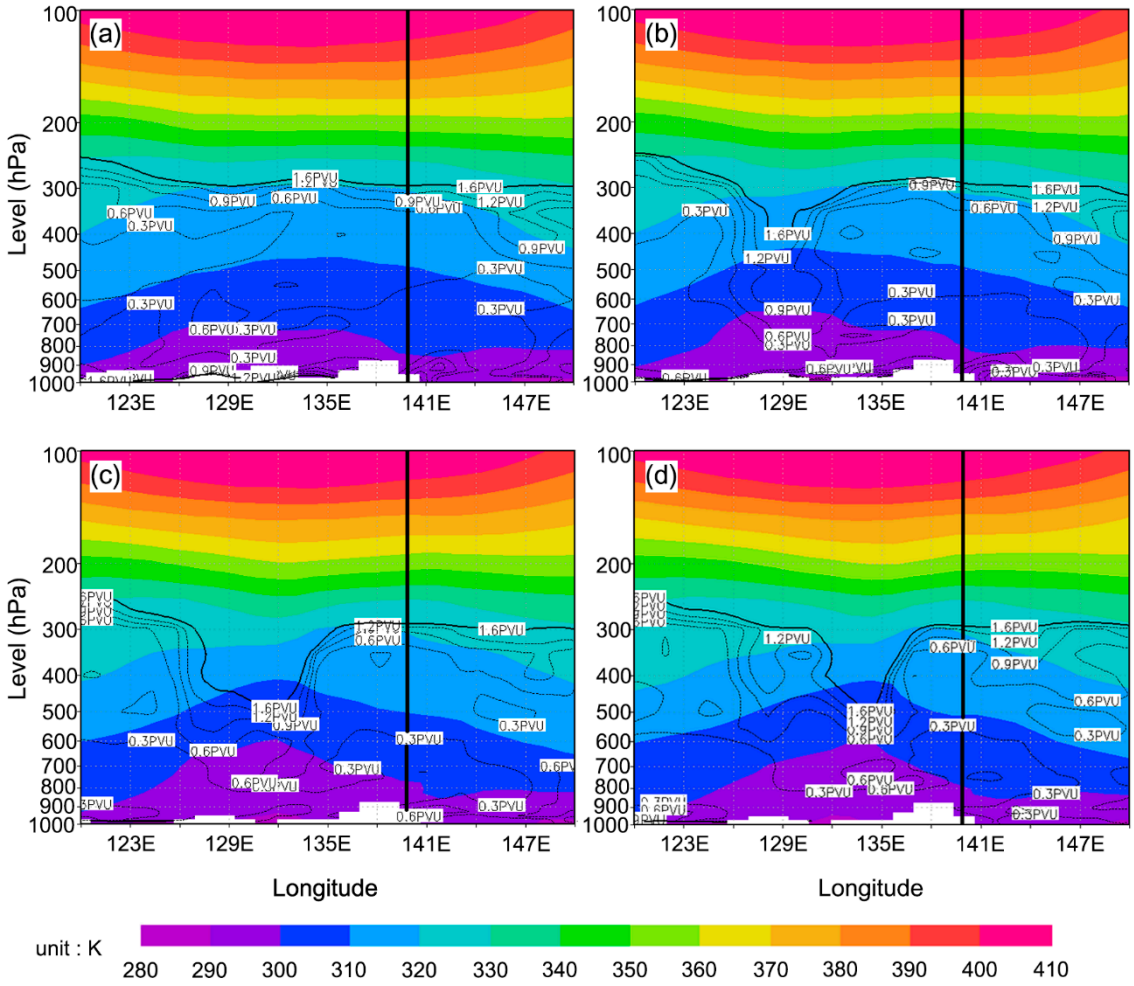

Figure 7. Vertical cross-section of the potential vorticity (PV, solid line) and potential temperature (dashed line) along 40°N for (a) 1800 UTC 5, (b) 2100 UTC 5, (c) 2100 UTC 5, and (d) 0300 UTC 6 May 2012, respectively. PV unit is in [10^{-6} m^2K $kg^{-1}s^{-1}$].

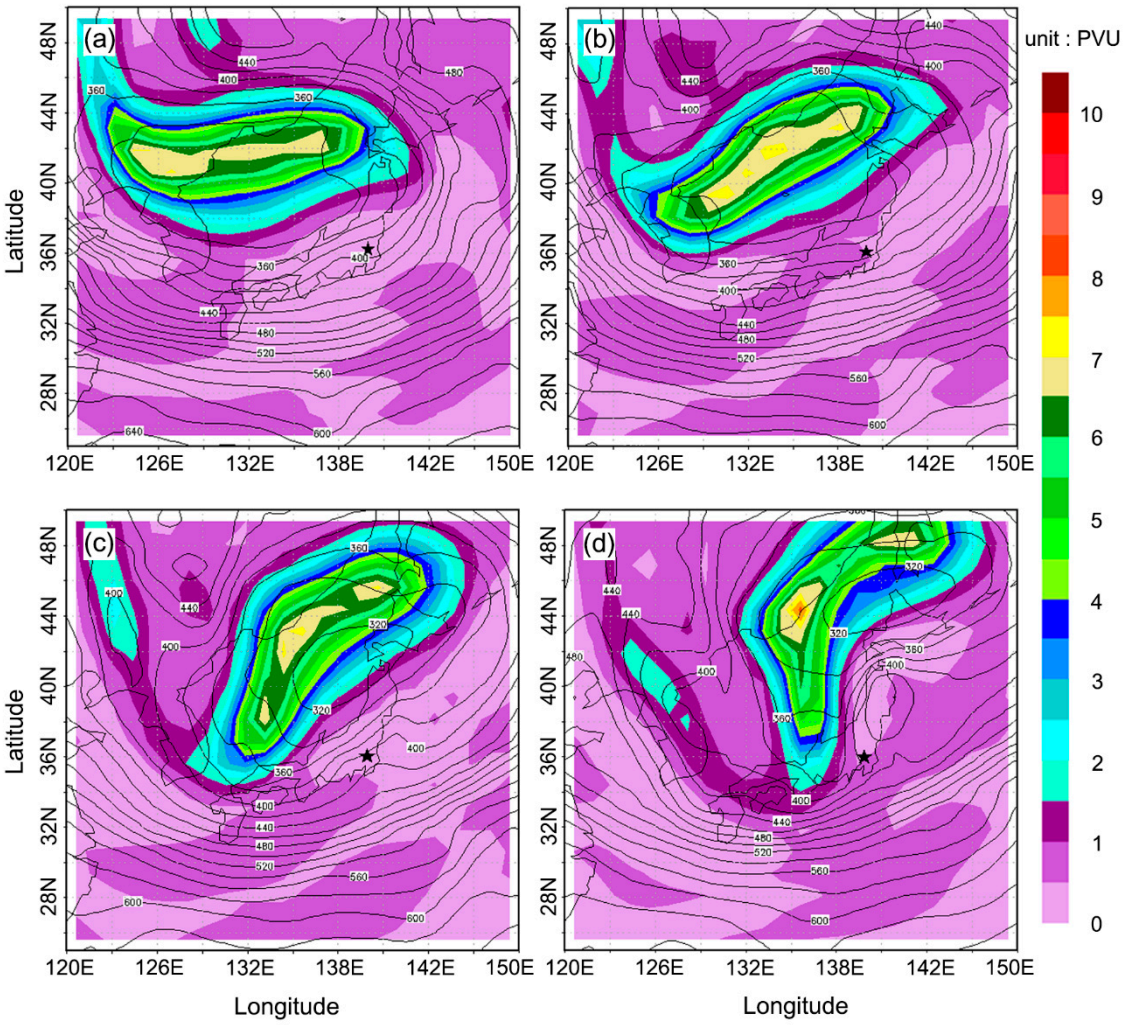

Figure 8. Isentropic analysis at the 315 K level with PV (short dashed line) for (a) 1200 UTC 5, (b) 1800 UTC 5, (c) 0000 UTC 6, and (d) 0600 UTC 6 May 2012, respectively. Long dashed line represents the pressure level. Thick solid line represents 1.5 PVU.

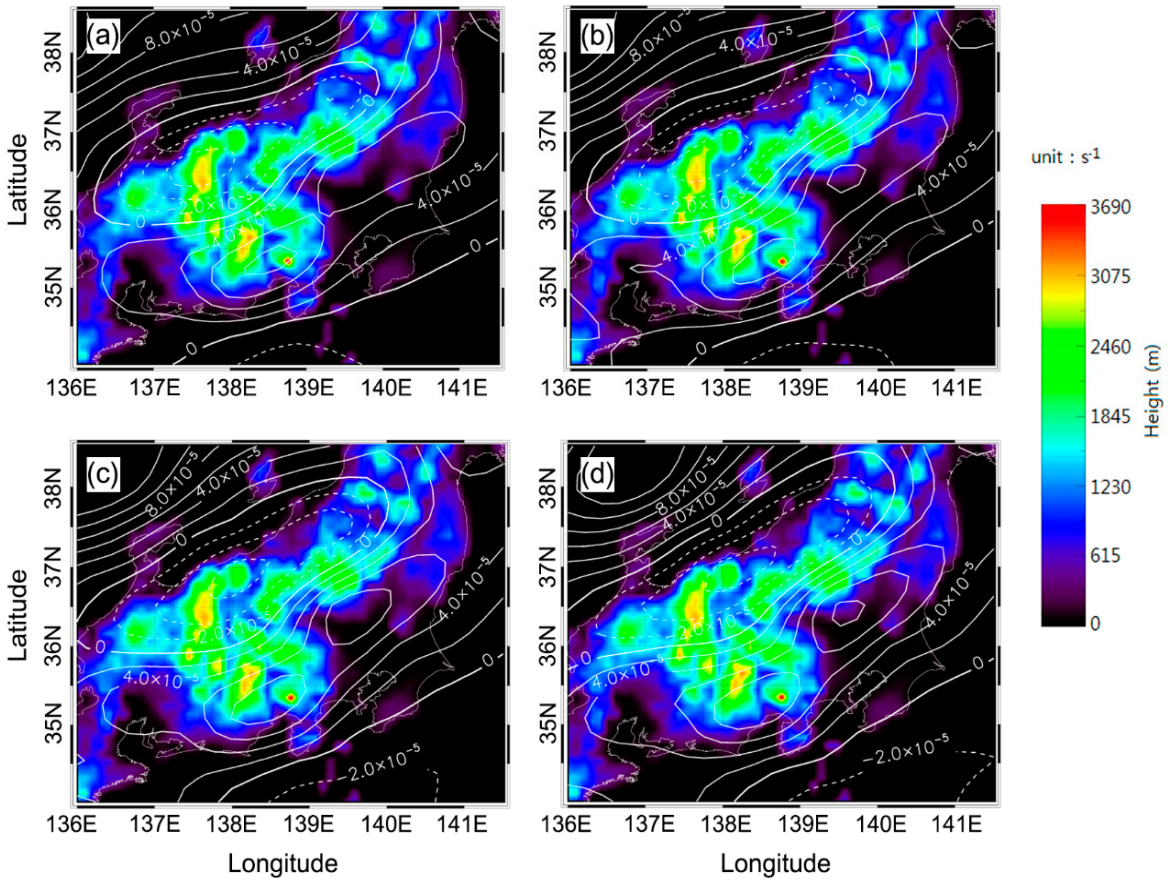

Figure 9. Vorticity at the 850 hPa level for (a) 0100 UTC (b) 0200UTC (c) 0300 UTC, and (d) 0400 UTC 6 May 2012, respectively. Solid and dashed lines represent cyclonic and anticyclonic vorticity with a contour interval at $2.0 \times 10^{-5}\ s^{-1}$. Color shading represents topography height.

Table 2. Froude number from 1500 UTC 05 to 0000 UTC 06 May 2012 at 35°N 137°E.

	1500UTC 5	1800UTC 5	2100UTC 5	0000UTC 6	0300 UTC 6
850 hPa	0.8	1	1.3	1.4	1.4
975~850 hPa	0.4	0.8	1.3	1.3	1.3

4. Summary and Conclusions

In this study, we examined the synoptic and mesoscale kinematic mechanisms on the formation and development of the Tsukuba tornado, which occurred on 6 May 2012. We used surface and upper-level weather charts, thermodynamic diagrams, hodographs, stability indices, moisture flux, SREH, isentropic analysis, PV, and Froude number for the analyses.

Synoptic analysis revealed that there was a circular jet stream over Japan before the tornado event and the surface was moist due to overnight precipitation. The 0000 UTC 6 May sounding showed a capping inversion at 900 hPa. Circular jet stream brought cold and dry air to the

upper-level and sky clearing with strong solar radiation heated the ground for a tornadic supercell to develop in an area that was potentially unstable. The stability indices at 0000 UTC 6 May 2012 also showed a favorable environment for supercell development. CAPE was 508.9 Jkg^{-1}, SWEAT 325.4, LI -2.74, and SSI -1.37, all indicating a moderate possibility of a severe thunderstorm with some chance for a tornado. The surface air temperature rose to 26℃ at 0300 UTC 06, breaking the cap and vigorous updraft with rotation due to the shear caused multiple tornadoes to occur from 0220 to 0340 UTC 6 May 2012.

From the results of the mesoscale analysis, we found that there was an influx of moisture from the adjacent Pacific Ocean and the equivalent potential temperature decreased from the surface to 600 hPa indicating a strong thermodynamic instability. In addition, there was a strong vertical shear of 20 ms^{-1} or more and a cyclonic vorticity of $1.0 \times 10^{-4}\ s^{-1}$ in the lower-level, and the value of SREH reached up to 480 m^2s^{-2} showing that the atmospheric environment was ripe for a tornado outbreak to occur. However, comparing Tateno's climatological profile of temperature and dew-point temperature with that of the day of the tornado outbreak showed that the mid-level had more moisture (3~4 ℃) than that of a typical tornado sounding. Thus, the cause of the tornado occurring in Tsukuba differs from that of the typical U.S. Great Plains tornado and the role of the upper-level dynamics and topography were investigated. A PV anomaly associated with tropopause folding approached Japan from the west before the tornado outbreak, and its intensity gradually increased, so cyclonic circulation was accelerated at the 850 hPa level. Furthermore, calculation of the Froude number, which was greater than 1 throughout the period of the Tsukuba tornado, indicated that the Japanese Alps acted as a mountain barrier that allowed a column of air to flow over and enhance the vortex by stretching the column, which had an effect on the tornado outbreak.

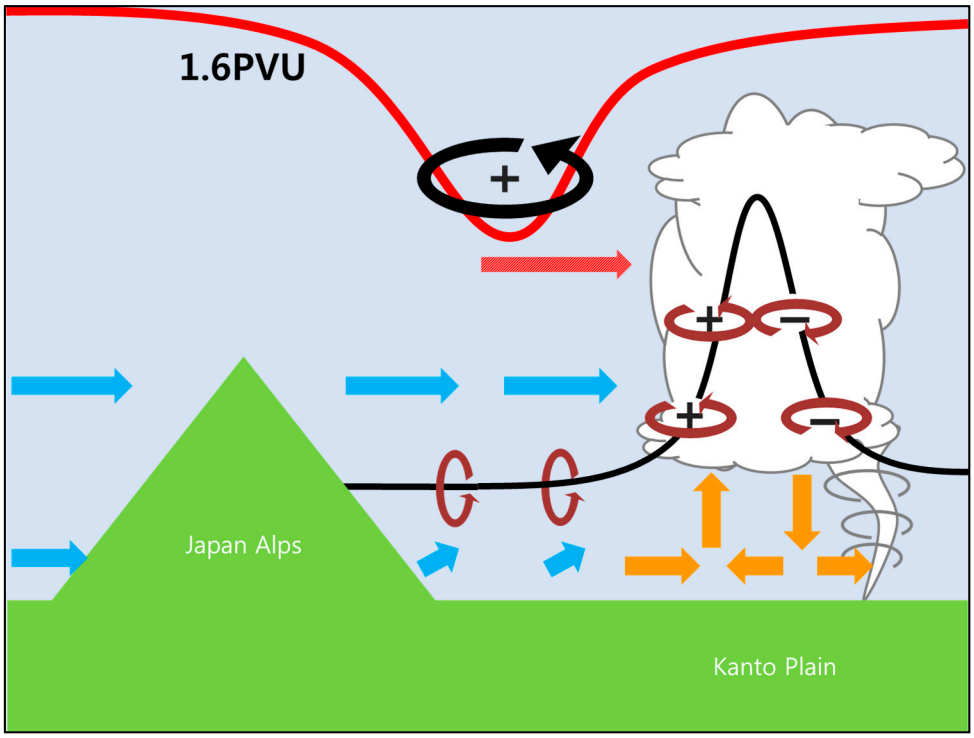

Fig. 10. Schematic diagram of Tsukuba tornado formation. The black lines are vortex lines, with the sense of rotation indicated by brown circular arrows with cyclonic (+) and anticyclonic (-) signs. The red line represents 1.6 PVU dynamic tropopause level, the red arrow represents the direction of PV advection, the blue arrows show 850 hPa and surface winds, and the orange arrows represent buoyant flow underneath the supercell.

Niino et al. [1] conducted a statistical study on tornado occurrence in Japan and found that the Kanto plain was the only region not located at the shore among regions where tornadoes intensively occurred. They hypothesized that tornados occurring in the Kanto plain may result from a topographical effect. Our study shows that the development of the Tsukuba tornado was due to not a single mechanism but a combination of mechanisms including 1) topography and PV anomaly, which increased the vorticity over the Kanto Plain, 2) vertical shear, which produced a horizontal roll like rotation or vortex line, and 3) thermal instability, which triggered a supercell and tilted the vortex line in the vertical direction (Figure 10). The overall synoptic development mechanism is similar to that of a U.S. Great Plains tornado but the mesoscale upper-level moisture structure and topographical effect were quite distinct in the case of the Tsukuba tornado.

Acknowledgments: This study is supported by the Korea Meteorological Administration Research and Development Program (Grant No. KMIPA 2015-1090).

Author Contributions: K.-H. Min and K.-E. Kim conceived and designed the experiments; S. Choo performed the experiments; K.-H. Min and S. Choo analyzed the data; G. Lee contributed reagents/materials/analysis tools; K.-H. Min wrote the paper.

Conflicts of Interest: "The authors declare no conflict of interest." "The founding sponsors had no role in the design of the study; in the collection, analyses, or interpretation of data; in the writing of the manuscript, and in the decision to publish the results".

Abbreviations

The following abbreviations are used in this manuscript:

CAPE: Convective Available Potential Energy
COMS: Communication, Ocean and Meteorological Satellite
EHI: Energy Helicity Index
ICAO: International Civil Aviation Organization
JMA: Japan Meteorological Agency
LI: Lifted Index
MERRA: Modern-Era Retrospective analysis for Research and Applications
PBL: planetary boundary layer
PV: Potential Vorticity
RFD: rear flank downdraft
SREH: Storm Relative Environmental Helicity
SSI: Showalter Stability Index
SWEAT: Severe WEAther Threat index

References

[1] Niino, H.; Fujitani, T.;Watanabe, N. A Statistical Study of Tornadoes and Waterspouts in Japan from 1961 to 1993. *J. of Climate*, **1997**, Volume 10, pp. 1730-1752.

[2] Matsuia, M.; Tmuraa, Y.; ShuyangCaob, A.Y.; Kobayashic, F.; Okadaa, R.; Sabareesha, G. Recent Tornado Damage in Japan. **2009**, 14 pp., Available online: http://www.iawe.org/WRDRR_Bangladesh/Preprints/S5TPU.pdf (accessed on 9 March 2017).

[3] Japan Meteorological Agency (JMA). Report of tornadoes occurred on 6 May 2012 (in Japanese). **2012**, 14 pp., Available online: http://www.jma.go.jp/jma/menu/tatsumakiportal/tyousa-houkoku.pdf], (accessed on 13 February 2017).

[4] Klemp, J.B.; Rotunno, R. A Study of the Tornadic Region within a Supercell Thunderstorm. *J. of Atmos. Sci*, **1983**, Volume 40(2), pp. 359-377.

[5] Davis, C.A.; Emanuel, K.A. Potential Vorticity Diagnostics of Cyclogenesis. *Mon. Wea. Rev.*, **1991**, Volume 119(8), pp. 1929-1953 .

[6] Kerr, B.W.; Darkow, G.L. Storm-Relative Winds and Helicity in the Tornadic Thunderstorm Environment. *Wea. Forecasting*, **1996**, Volume 11(4), pp. 489-505.

[7] Takayabu, I.; Niino, H.; Yamanaka, M.; Fukao, S. An Observational Study of Cyclogenesis in the lee of the Japan Central Mountains. *Meteor. Atmos. Phys.*, **1996**, Volume 61, pp. 39-53.

[8] Brooks, H.E.; Lee, J.W.; Craven, J.P. The Spatial Distribution of Severe Thunderstorm and Tornado Environments from Global Reanalysis Data. *Atmos. Res.*, **2003**, Volume 67, pp. 73-94.

[9] Noda, A. T.; Niino, H. Genesis and Structure of a Major Tornado in a Numerically-Simulated Supercell Storm: Importance of Vertical Vorticity in a Gust Front. *Sci. Online Letters Atmos.*, **2005**, Volume 1, pp. 5-8.

[10] Verbout, S.M.; Brooks, H.E.; Leslie, L.M.; Schultz, D.M. Evolution of the U.S. Tornado Database: 1954-2003. *Wea. Forecasting*, **2006**, Volume 21, pp. 86-93.

[11] Gold, D.A.; Nielsen-Gammon, J.W. Potential Vorticity Diagnosis of the Severe Convective Regime. Part IV: Comparison with Modeling Simulations of the Moore Tornado Outbreak. *Mon. Wea. Rev.*, **2008**, Volume 136, no.5, pp. 1612-1629.

[12] Seko, H.; Saito, K.; Kunii, M.; Kyouda, M. Mesoscale Ensemble Experiments on Potential Parameters for Tornado Outbreak. *Sci. Online Letters Atmos.*, **2009**, Volume 5, pp. 57-60.

[13] Sato, E.; Yamauchi, H.; Mashiko, W.; Shoji, Y.; Suzuki, O. Multiple Doppler analysis of the Tsukuba tornado on May 6, 2012. Proceedings of the 26th Conference on Severe Local Storms, Nashville, TN, U.S.A., **2012**, pp. 7-10.

[14] Rienecker, M.M.; Suarez, M.J.; Gelaro, R.; Todling, R.; Bacmeister, J.; Liu, E.; Bosilovich, M.G.; Schubert, S.D.; Takacs, L.; Kim, G.-K.; Bloom, S.; Chen, J.; Collins, D.; Conaty, A.; da Silva, A. et al. MERRA: NASA's Modern-Era Retrospective Analysis for Research and Applications. *J. Climate*, **2011**, Volume 24(14), pp. 3624-3648.

[15] Niino, H.; Suzuki, O.; Nirasawa, H.; Fujitani, T.; Ohno, H.; Takayabu, I.; Kinoshita, N.; Ogura, Y. Tornadoes in Chiba prefecture on 11 December 1990. *Mon. Wea. Rev.*, **1993**, Volume 121(11), pp. 3001-3018.

[16] Markowski, P.; Richardson, Y. *Mesoscale Meteorology in Midlatitudes*; Wiley-Blackwell, New York, U.S.A., **2010**, 274 pp.

[17] Reed, R. J. A Study of a Characteristic Type of Upper-Level Frontogenesis. *J. Applied Meteor. and Climato.*, **1955**, Volume 12, no. 3, pp. 226–237.

[18] Hoerling, M.P.; Schaack, T.K.; Lenzen, A.J. Global Objective Tropopause Analysis. *Mon. Wea. Rev.*, **1991**, Volume 119(8), pp. 1816-1831.

[19] Bithell, M.; Gray, L.J.; Cox, B.D. A Three-Dimensional View of the Evolution of Midlatitude Stratospheric Intrusions. *J. Atmos. Sci.*, **1999**, Volume 56, no. 5, pp. 673-688.

[20] Kim, J.Y.; Min, K.-H.; Kim, K.-E.; Lee, G.-W. A Case Study of Mesoscale Snowfall Development Associated with Tropopause Folding (in Korean). *Atmosphere*, **2013**, Volume 23(3), pp. 331-346.

[21] Davies, J.M. Tornadoes with Cold Core 500-mb Lows. *Wea. Forecasting*, **2006**, Volume 21, no. 6, pp. 1051-1062.

[22] Petty, W.G. *A First Course in Atmospheric Thermodynamics*; Sundog Publishing, Madison, U.S.A., **2008**, 352 pp.

[23] Shimizu, S.; Uyeda, H.; Moteki, Q.; Maesaka, T.; Takaya, Y.; Akaeda, K.; Kato, T.; Yoshizaki, M. Structure and Formation Mechanism on the 24 May 2000 Supercell-Like Storm Developing in a Moist Environment over the Kanto Plain, Japan. *Mon. Wea. Rev.*, **2008**, Volume 136, no. 7, pp. 2389-2407.

[24] Bunkers, M.J.; Klimowski, B.A.; Zeitler, J.W.; Thompson, R.L.; Weisman, M.L. Predicting Supercell Motion Using a New Hodograph Technique. *Wea. Forecasting*, **2000**, Volume 15(1), pp. 61-79.